Inverse-Designed Photonic Polarization Control for High-Density Integration on Foundry Platforms

A. Khurana, J. B. Slaby, A. M. Hammond[†] and S. E. Ralph^{*}

School of ECE, Georgia Institute of Technology, 30318, Atlanta GA, USA *stephen.ralph@ece.gatech.edu

Abstract—Compact, wideband structures to enable chip-scale polarization control are essential elements for large-scale integrated photonics. We experimentally validate inverse-designed polarization control structures fabricated on a commercial foundry, demonstrating rotator conversion efficiency of -1.5dB and splitter insertion losses of 1.4dB (TE) and 2.6dB (TM) across C-band.

Keywords — inverse design, polarization, splitter, rotator

I. INTRODUCTION

Harnessing the scalability and density potential of silicon photonics platforms requires compact, versatile components that can generate, process, and detect all the degrees of freedom of optical signals. Indeed, these functions are essential for advanced telecom, sensing, and quantum applications [1]. A key advantage of photonics is the polarization degree of freedom. This enables, for example, multi-dimensional direct detection using a Stokes vector receiver [2] and polarizationmultiplexed signaling such as that found in digital coherent detection. Notably, conventional photonic components may not maintain interoperability between systems because they are often custom designed for a particular application. Using topology optimization, an inverse design methodology [3], we designed a family of polarization control elements. Here we detail the design process and experimentally demonstrate compact, fully interoperable, photonic polarization rotators and splitters that enable broadband, low-loss, high-density chipscale polarization control. All devices were fabricated on the GlobalFoundries (GF) 45CLO process.

II. DESIGN AND OPTIMIZATION

We employ a hybrid time-frequency domain topology optimization methodology. The broadband time-domain fields are simulated in Meep [4] and accumulated in a discrete-time Fourier transform. Using the adjoint variable method, the frequency-domain response is used to inject an adjoint source into the device and back-propagate through all degrees of freedom (permittivity voxels), freely evolving the topology of the device to maximize one or more user-specified objective functions while satisfying foundry design rule check (DRC) constraints [5]. Importantly, both the polarization rotator and splitter utilize two layers of the GF process. The inset in Fig. 1. shows the multi-layer structure of the polarization rotator. The silicon layer (blue) is co-optimized with the polysilicon layer (gold), while satisfying DRC for each layer independently [5]. Multi-layer optimization allows for a far greater number of degrees of freedom, increased modal confinement, and the

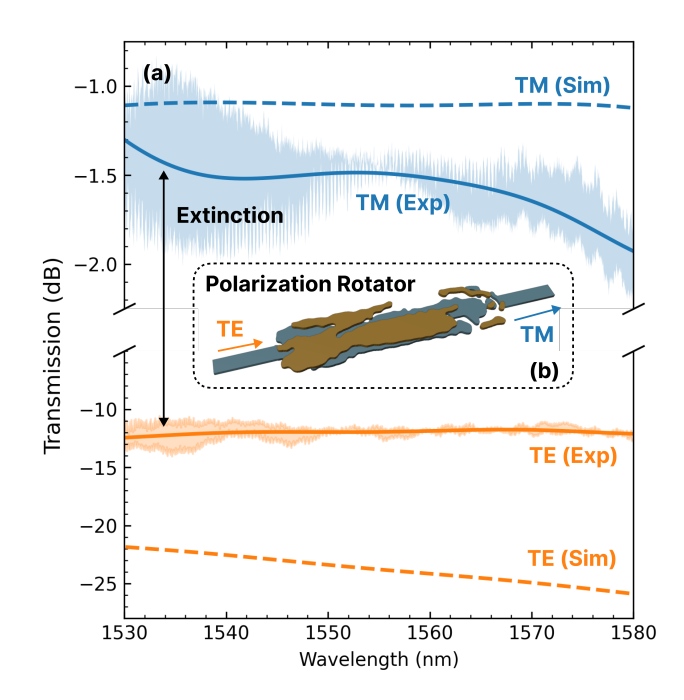


Fig. 1. (a) Simulated (dashed) and measured, smoothed (solid) transmission of TE and TM modes through the polarization rotator. The shaded region indicates variability of experimental result across two measured devices. (b) 3D render of the optimized device topology with silicon (blue) and polysilicon (gold) layers.

breaking of z-symmetry. These are essential to maintaining the compact nature of the device.

We designed a compact (8 μm x 2 μm) polarization rotator for operation across C-band. In the forward operation condition, the device rotates the fundamental quasi-transverse-electric (TE₀₀) mode to the fundamental quasi-transverse-magnetic (TM₀₀) mode. In the reverse operation condition, the TM₀₀ mode is rotated to the TE₀₀ mode.

We also designed a compact (5 μm x 5 μm) polarization splitter using a multi-objective optimization technique to simultaneously optimize for the performance in the TE and TM operation conditions. In forward operation the fundamental TE and TM modes of the input waveguide are routed to separate waveguides with high extinction. The fundamental output modes retain their polarization, i.e., TE remains TE and TM remains TM. In reverse operation the device can be used to combine two distinct polarizations into a single guide. Therefore, a combined TE/TM signal can be demultiplexed and

^{†.} Now with Reality Labs, Meta Platforms, Inc.

routed to separate waveguides while maintaining their respective modes. This is distinct from conventional polarization splitter-rotators, (PSRs), which couple both TE/TM inputs to TE output modes during forward operation and require two TE inputs in reverse operation. Our two interoperable devices combine to form polarization-agnostic structures.

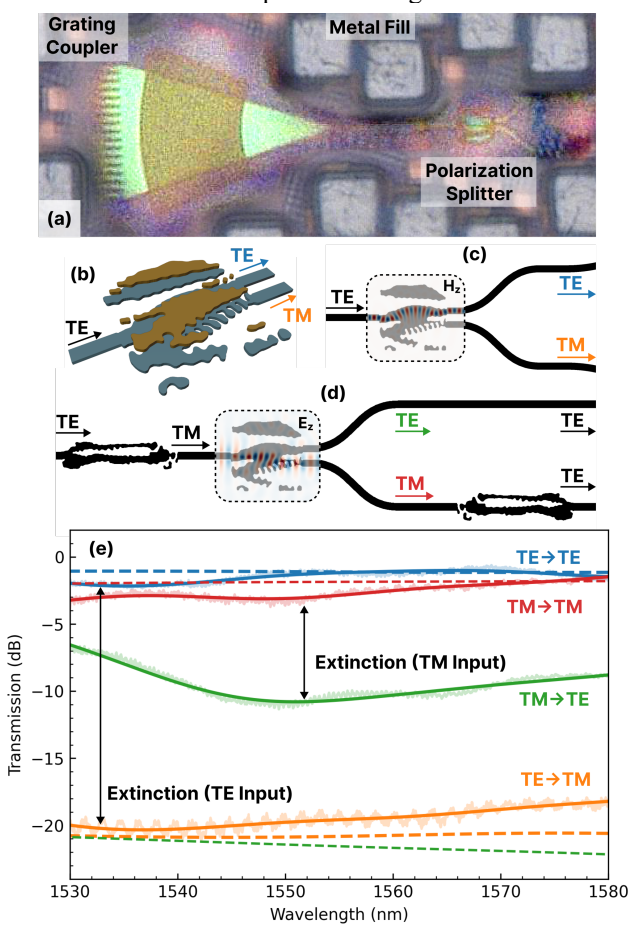


Fig 2. (a) Optical micrograph of the polarization splitter. (b) 3D render. (c-d) Test structures with overlaid fields. (e) Simulated (dashed) and measured, smoothed (solid) transmission of fundamental TE/TM modes. The shaded region indicates the raw (normalized) data.

III. EXPERIMENTAL RESULTS

The devices were experimentally evaluated using a high-dynamic range Koheron logarithmic photodiode. The laser source was swept from 1530 nm to 1580 nm. Conversion efficiency (CE) of the polarization rotator was characterized as the transmission of the fundamental TM mode through the device in the forward operation condition. Figure 1a compares the simulated and measured results for the polarization rotator. The rotator has an average CE of -1.5 dB across the optimization band. The transmission of the fundamental TE mode during forward operation was measured to be -12.0 dB. Thus, the polarization extinction ratio (ER) is ~10.5 dB. Reciprocity demands that this CE and ER hold in the reverse operation condition.

Figure 2e compares measured and simulated results for the polarization splitter. For the TE operation evaluation of the

polarization splitter, incident light from the grating coupler enters the input port of the polarization splitter. The light is routed to the top output port, and the output power is measured. In the TE operation, the splitter is measured to have an average insertion loss (IL) of 1.4 dB, and an average ER between the two output ports of 18.0 dB. For the TM operation, additional test structures are necessary. We utilize the polarization rotator described in the previous section to convert the incident light from the grating coupler to the fundamental TM mode. The light then propagates through the splitter and is routed to the bottom output port. For measurement purposes, the light is rotated back to the TE waveguide mode using the reverse operation condition of the polarization rotator. In the TM operation, the splitter is measured to have IL of 2.6 dB, and an average ER of 7.0 dB. The imperfect CE of the polarization rotator causes leakage of the TE mode into the splitter in the TM operation condition, leading to increased power at the output TE port and a degraded measured ER in this case.

IV. CONCLUSION

Using an inverse design methodology, we designed and subsequently fabricated multiple polarization control structures on a commercial silicon photonics foundry platform. Devices were experimentally demonstrated to perform as designed. The polarization rotator was shown to have -1.5 dB average CE and 10.5 dB ER. The polarization splitter was shown to have IL of 1.4 dB in the TE mode (18.0 dB ER) and 2.6 dB in the TM mode (7.0 dB ER). The input-agnostic nature of the polarization splitter ensures full interoperability of each component presented with other photonic subsystems. This work demonstrates that compact polarization control structures are readily fabricated on commercial platforms enabling large-scale high-density polarization-sensitive photonic systems.

ACKNOWLEDGMENT

This research was supported in part through the Partnership for an Advanced Computing Environment (PACE) at the Georgia Institute of Technology. This material is based upon work supported in part by the National Science Foundation (NSF) Center "EPICA" under Grant No. 2052808, https://epica.research.gatech.edu. Any opinions, findings, and conclusions or recommendations expressed in this material are those of the author(s) and do not necessarily reflect the views of the NSF.

REFERENCES

- [1] Rickman, A. The commercialization of silicon photonics. *Nature Photon* **8**, 579–582 (2014). https://doi.org/10.1038/nphoton.2014.175
- [2] Hammond, A.M., et. al., (2022). Photonic Inverse Design of Compact Stokes-Vector Receiver on Commercial Foundry Platforms. In 2022 European Conference on Optical Communications (ECOC) (pp.1-4).
- [3] Hammond, A.M., et. al., "High-performance hybrid time/frequency-domain topology optimization for large-scale photonics inverse design," Opt. Express 30, 4467-4491 (2022).
- [4] Oskooi, A.F., et. al., "Meep: A flexible free-software package for electromagnetic simulations by the FDTD method", Computer Physics Communications, Volume 181, Issue 3, 2010, Pages 687-702.
- [5] Hammond, A.M, et. al., "Photonic topology optimization with semiconductor-foundry design-rule constraints," Opt. Express 29, 23916-23938 (2021).